Journal of Advanced Research (2016) 7, 1009–1017

Cairo University

Journal of Advanced Research

ORIGINAL ARTICLE

Low-cost composites based on porous titania–apatite surfaces for the removal of patent blue V from water: Effect of chemical structure of dye

C. El Bekkali [a], H. Bouyarmane [a], S. Saoiabi [a], M. El Karbane [b], A. Rami [b], A. Saoiabi [a], M. Boujtita [c], A. Laghzizil [a,*]

[a] *Laboratoire de Chimie Physique Générale, Faculté des Sciences, Université Mohammed V, Av. Ibn Batouta, B.P. 1014 Rabat, Morocco*
[b] *Laboratoire National du Contrôle des Médicaments, Rue Lamfaddal Cherkaoui, B.P. 6206 Rabat, Morocco*
[c] *Chimie Interdisciplinarité: Synthèse, Analyse, Modélisation CNRS (CEISAM), Faculté des Sciences et Techniques, Université de Nantes – UBL, B.P. 92208, 44322 Nantes Cedex 03, France*

GRAPHICAL ABSTRACT

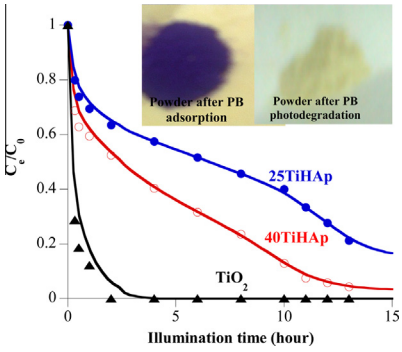

* Corresponding author. Fax: +212 537 77 54 40.
E-mail address: laghzizi@fsr.ac.ma (A. Laghzizil).
Peer review under responsibility of Cairo University.

Production and hosting by Elsevier

http://dx.doi.org/10.1016/j.jare.2016.05.001

ARTICLE INFO

Article history:
Received 7 February 2016
Received in revised form 5 May 2016
Accepted 6 May 2016
Available online 12 May 2016

Keywords:
Apatite/titania
Patent blue
Adsorption
Degradation
Photocatalysis
Kinetic modeling

ABSTRACT

Hydroxyapatite/titania nanocomposites (TiHAp) were synthesized from a mixture of a titanium alkoxide solution and dissolution products of a Moroccan natural phosphate. The simultaneous gelation and precipitation processes occurring at room temperature led to the formation of TiHAp nanocomposites. X-ray diffraction results indicated that hydroxyapatite and anatase (TiO_2) were the major crystalline phases. The specific surface area of the nanocomposites increased with the TiO_2 content. Resulting TiHAp powders were assessed for the removal of the patent blue V dye from water. Kinetic experiments suggested that a sequence of adsorption and photodegradation is responsible for discoloration of dye solutions. These results suggest that such hydroxyapatite/titania nanocomposites constitute attractive low-cost materials for the removal of dyes from industrial textile effluent.

Introduction

Various water treatment processes have been reported in the literature including advanced oxidation, membrane filtration, biological degradation, electrochemical oxidation, photocatalytic degradation, and adsorption [1–3]. Among these, adsorption has the advantage of simplicity and can be achieved using a wide range of low-cost sorbents that can be easily regenerated after use [4]. For instance, natural phosphate and its derivative apatite have attracted large interest for the removal of organic and inorganic pollutants due to their reactive surface and ion-exchange capacity [5–7].

However, natural phosphates usually exhibit low specific surface area limiting their sorption capacity. To address this point, we have previously reported a simple route to convert the natural phosphate into a mesoporous hydroxyapatite via a dissolution/precipitation method [6]. Further improvement of the sorption capacity of these converted phosphates could be achieved via surface functionalization using phosphonate or aminophosphonate species [7,8]. However, calcium phosphate minerals do not possess significant photocatalytic properties.

A promising approach to confer photodegradation capability to calcium phosphates relies on their association with titania (TiO_2) whose photocatalytic properties have been widely studied [3,9,10]. Several synthetic approaches such as sol–gel chemistry [11], hydrothermal conditions [12] and microwave irradiation [13] have been used to obtain such HAp/TiO_2 nanocomposites. Recently, we have described a novel process based on the gelation/precipitation of TiO_2–HAp (named TiHAp) nanocomposites using ultrasound irradiation [14]. This process has the advantage of using natural phosphate as a starting raw material therefore providing a low-cost route to composite adsorbents that showed excellent performances for the removal of methylene blue (MB) from aqueous solutions [14]. These studies enlightened the strong influence of the dye structure on its interactions with both apatite and TiO_2, in agreement with the literature [15–18]. To extend our understanding of these interactions and evaluate the potentialities of these nanocomposites for the removal of a wider range of dyes, we have here studied the capacity of TiHAp nanomaterials to remove the patent blue V dye from water. The nanocomposite surface reactivity and removal efficiency toward patent blue V and methylene blue have been compared in order to elucidate the mechanisms being the dual sorption/photodegradation phenomena and predict possible extension of this process to other organic pollutants.

Experimental

Adsorbent-photoactive wTiHAp nanocomposites

The natural phosphate (NP) originates from the Bengurir region (Morocco). The converted hydroxyapatite (HAp) powders were prepared with NP by using a dissolution–precipitation method reported elsewhere [6]. The phosphate rock was first dissolved in a nitric acid solution to obtain Ca^{2+} and H_3PO_4 species. After separation of the insoluble matter by filtration, the remaining solution was neutralized by a concentrated NH_4OH solution (25%) and the mixture was placed in an ultrasonic water bath sonicator (35 kHz) for 30 min. The resulting precipitate was recovered by filtration and re-suspended in deionized water under stirring for 30 min and under sonication for 30 min more. Finally, the product was filtered, washed with deionized water and dried overnight at 100 °C. The TiO_2 powder was synthetized via a sol–gel method using a tetraisopropyl orthotitanate solution (TIPT) (99%, Sigma–Aldrich, France) in 1-propanol and NH_4OH (25 wt.% in water). The two solutions were mixed under stirring for 24 h. The resulting precipitate was filtered, thoroughly washed with deionized water, re-dispersed in water under sonication for 30 min and filtered again. The final gel was dried overnight at 100 °C. TiHAp nanocomposites were prepared by mixing the dissolved natural phosphate solution containing Ca^{2+} and H_3PO_4 species with the TIPT solution under sonication, followed by ammonia addition. The resulting gel-like solid was washed and dried following the above-described procedure. In some cases, the TiHAp powders were thermally treated at 500 °C and 800 °C overnight. Samples were named wTiHAp with weight ratio w = TiO_2:HAp (w = 25 and 40).

Dye-sorption experiments

Patent blue (PB) and methylene blue (MB) were purchased from Sigma–Aldrich Chemie GmbH (Munich, Germany) and used without further purification. PB dye solutions with concentrations ranging from 0 to 50 mg L^{-1} were prepared

in distilled water. The concentration range was selected based on several preliminary investigations and in accordance with the levels of these hazardous species present in wastewater/industrial effluents. A 200 mg of adsorbent was added to dye solutions (100 mL), and magnetically stirred at room temperature. For each selected aging time t, the suspensions were sampled and centrifuged. No adjustment of the solution pH was undertaken during the sorption experiments in order to simulate natural conditions. The residual dye concentration was analyzed using a UV visible spectrophotometer (Perkin Elmer Lambda 35, Waltham, Massachusetts, USA) and controlled by HPLC technique (Alliance HPLC system, Massachusetts, USA) equipped with barrette Diode PDA2998 with an Inertsil C18 column (250 × 4.6 mm) and 5 μm particle size coupled to UV absorption detector. All provided experimental data are the average of triplicate determinations, and the relative errors are about 5%. The amount of adsorbed dye per gram of wTiHAp adsorbent q_t (in mg g^{-1}) at time t was calculated as follows:

$$q_t = \frac{C_0 - C_t}{w} \cdot V \quad (1)$$

where q_t is the amount of adsorbed dye at time t (mg g^{-1}), C_0 and $C(t)$ are the dye concentration in solution at $t = 0$ and $t = t$ (mg L^{-1}), V is the volume (L) of the dye solution and "w" is the weight (g) of the adsorbent. Kinetic parameters of the PB sorption on wTiHAp were determined in batch experiments at room temperature using 200 mg of adsorbent in contact with 100 mL of an aqueous solution containing 20 mg L^{-1} of the dye. In order to determine the rate constants, the two most widely used kinetic models in sorption processes (pseudo-first and pseudo-second order models) have been applied to experimental data. The Lagergren pseudo-first order equation can be written as [19]

$$\log(q_e - q_t) = \log q_{e,1} - \frac{k_1}{2.303} t \quad (2)$$

where q_e and $q_{e,1}$ are the experimental and calculated amount of adsorbed dye at equilibrium (mg g^{-1}) and k_1 the first order kinetic constant (min^{-1}). This model can be applied if $\log(q_e - q_t)$ versus t gives a straight line, in which case $q_{e,1}$ and k_1 can be calculated from the intercept and slope of the plot. The pseudo-second order model can be expressed as [20]

$$\frac{t}{q_t} = \frac{1}{k_2 q_{e,2}^2} + \frac{1}{q_{e,2}} t \quad (3)$$

where $q_{e,2}$ is the calculated amount of adsorbed dye at equilibrium (mg g^{-1}) and k_2 the second order kinetic constant (g mg^{-1} min^{-1}).

Adsorption isotherms onto solids studied were analyzed using the non-linear fitting of experimental points with the Langmuir and Freundlich equations. The Langmuir equation can be written as

$$\frac{C_e}{q_e} = \frac{1}{\beta \cdot q_L} - \frac{C_e}{q_L} \quad (4)$$

where C_e (mg L^{-1}) is the dye concentration at equilibrium, q_e (mg g^{-1}) is the adsorption capacity, q_L (mg g^{-1}) is the maximum adsorption capacity, and β (L mg^{-1}) is the Langmuir constant related to the free energy of adsorption.

The Freundlich model can be written as

$$q_e = K_f C_e^{1/n} \quad (5)$$

where K_f and n are Freundlich constants, correlated to the maximum adsorption capacity and adsorption intensity, respectively. A linear form of this model is: $\log q_e = \log K_f + 1/n \log C_e$.

Photodegradation experiments

The photocatalytic degradation of patent blue under a 125W UV A-B-C (200–600 nm) irradiation in the presence of wTiHAp powders heated at 500 °C was carried out using a home-made Pyrex helical photoreactor of 250 mL (Fig. 1). The source of irradiation was placed in the center of the reactor to insure the maximum energy exchange between the source of the irradiation and the reaction mixture that flows out continuously. Two tubular compartments surrounding the lamp were used for cooling system. Based on the previous kinetics sorption studies, the wTiHAp suspensions (200 mg) were constantly stirred for 30 min in the dark before irradiation to reach adsorption equilibrium. During the irradiation, the photoreactor was maintained under magnetic stirring to keep a homogeneous suspension, and promotes diffusion of the dyes to the solid surface. At each selected time, the suspensions were centrifuged at 4000 rpm for 20 min, and the supernatants were stored in the dark. The Langmuir–Hinshelwood (L–H) model was used to analyze the heterogeneous reactions occurring on the surface of catalysts. The rate law derived from the model was approximated by a simpler "pseudo-first order" model [21,22] represented by $\log \frac{C}{C_0} = -\frac{k_{app}}{2.303} t$, where C_0 is the initial concentration and k_{app} the apparent reaction constant.

Results and discussion

Characterization

Fig. 2 shows the typical XRD patterns of wTiHAp powders recorded on a Philips PW131 diffractometer, analytical Device using Cu Kα radiation. Dried powders exhibit broad diffraction peaks characteristic of a poorly crystalline hydroxyapatite structure. However, no clear diffraction peak corresponding to TiO_2 could be obtained, even for the 40TiHAp composite.

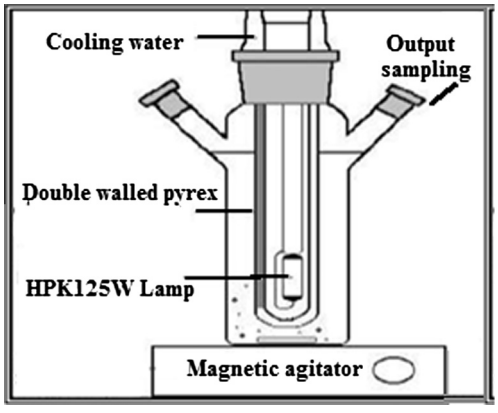

Fig. 1 Simplified schema of photo-reactor used in this study.

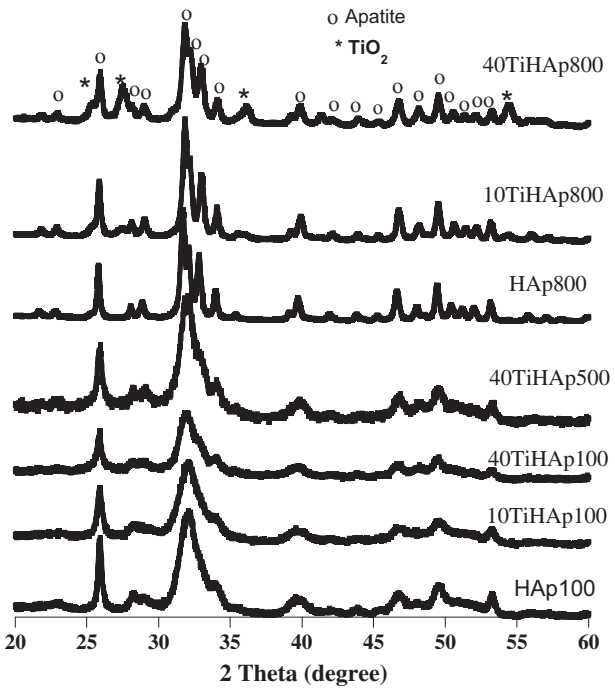

Fig. 2 X-ray diffractograms of the wTiHAp composite powders heated at 100 °C, 500 °C and 800 °C.

Heating at 500 °C for 3 h did not significantly improve hydroxyapatite crystallinity nor allowed for the detection of a crystalline form of titania. In contrast, after treatment at 800 °C, much narrower diffraction peaks corresponding to a well-crystallized HAp structure were evidenced and the presence of TiO_2 with an anatase structure could be identified in the 40TiHAp composite. To conserve their porosity, we limited the thermal treatment at 500 °C in valorizing their surface properties. The specific surface areas of these powders are accessed by multi-point N_2 gas sorption experiments at 77 K using a Micromeritics ASAP 2010 instrument (Aachen, Germany). As shown in Table 1, the specific surface area (S_{BET}) of the dried powders increases with TiO_2 content. The analysis of the pore size distribution shows that a main pore size of 11 nm starts from HAp with a second pore population at 3.5 nm for 40TiHAp. Thermal treatment of wTiHAp composites at 500 °C leads to a little reduction of S_{BET} values with a dramatic decrease in surface area obtained for TiO_2, while 40TiHAp material exhibits a larger S_{BET} value (225 $m^2 g^{-1}$) compared to other wTiHAp and TiO_2 powders. A significant increase in oxide content is obtained when the sample is previously heated. This result can be explained on the basis of the dehydroxylation of titania, followed by its conversion to the TiO_2-anatase with a negative charge at its surface [23]. Consequently, the precipitation of TiO_2 with HAp provides a better special repartition of the hydroxyapatite particles resulting thus in novel porous structure involving HAp-oxide interparticle voids [23]. Upon heating, the systematic decrease in specific surface area and the increase in pore size indicate the growth of both particles HAp and titania particles. However, the heat treatment of wTiHAp catalysts has a great influence on their surface properties, so a highest specific surface area is obtained with the material prepared by using 40TiHAp powder. However, the heat of wTiHAp powders at 800 °C leads to a dramatic loss of specific surface area, which their values do not reach 40 $m^2 g^{-1}$. Elemental analyses are conducted using inductively coupled plasma atomic emission spectroscopy (ICP-AES) with ICPS-7500 Shimadzu-France as the analytical device. Using unvarying Ca and P contents dissolved from phosphate rock as calcium and phosphorus precursors, the added Ti alkoxide could be distributed based on Ca/P molar ratio of the precipitates. It is confirmed that the Ti content in the final powder increases linearly with the amount of introduced Ti alkoxide (Table 1). It is worth noticing that in the case of 40TiHAp, a corresponding theoretical Ti/Ca molar ratio equal to 0.3 has been found.

Sorption of patent blue by wTiHAp nanocomposites

In order to investigate in detail the surface properties of wTiHAp nanocomposites, patent blue is selected not only due to its environmental relevance but also to study the effect of charge, size, structure, and relative affinities toward apatite and titania. Firstly, the effect of contact time on the adsorption of PB by wTiHAp nanocomposites is investigated to determine the adsorption saturation time (Fig. 3). A two-step mechanism occurs. The first step indicates that a rapid adsorption occurs during the first 30 min, after which the equilibrium is slowly reached. Therefore, 3 h period is taken as aging time for studying adsorption isotherms. The pseudo-first order and the pseudo-second order models have been applied to support the experimental data and to evaluate the kinetic parameters (Table 2). The R^2 values and the illustrated fits in Fig. 3 demonstrate that the pseudo-second-order model agrees with the experimental data, similar to the case of methylene blue (MB) [14], while the pseudo first order model does not depict a reliable agreement with the experimental data.

In order to describe the interaction between adsorbate and adsorbent, the adsorption isotherm has been investigated. The effect of initial concentration of patent blue is shown in Fig. 4 and indicates that the maximum adsorption capacity depends

Table 1 Elemental analyses, specific surface area and pore diameter at 100 °C and 500 °C.

Samples	Ca/P	Ti/Ca	S_{BET} ($m^2 g^{-1}$)		Pore diameter D_p (nm)	
			100 °C	500 °C	100 °C	500 °C
HAp	1.89	–	165	105	12	11
5TiHAp	1.81	0.04	205	145	3.5 and 11.5	4 and 9
10TiHAp	1.80	0.038	225	150	3.5 and 11.5	4 and 9
25TiHAp	1.67	0.21	260	185	3.5 and 9	4 and 9
40TiHAp	1.63	0.34	250	225	3.5 and 9	4 and 9
TiO_2	–	–	280	155	3.5	5.5

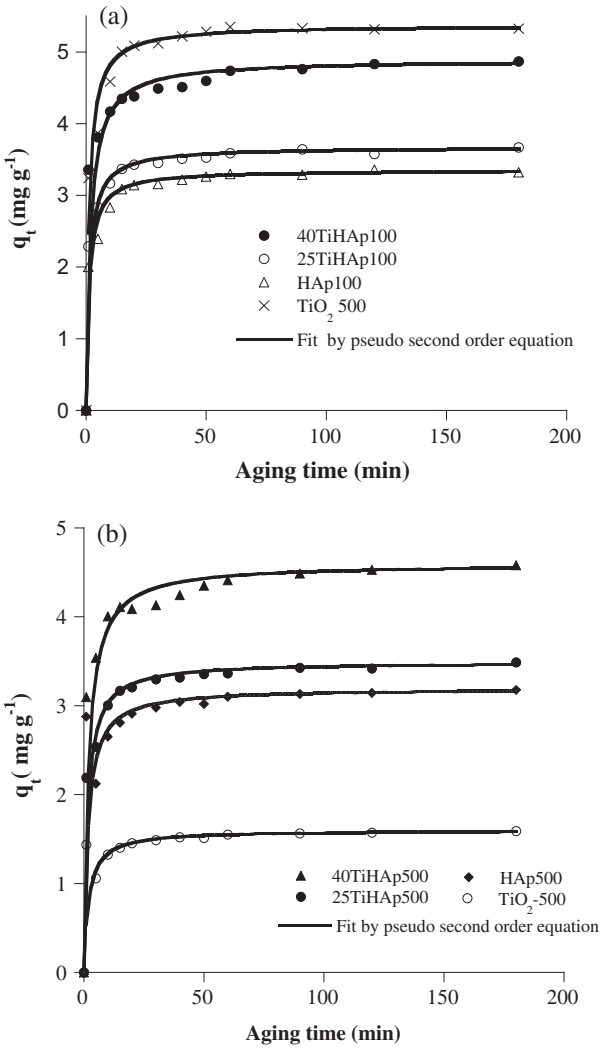

Fig. 3 Effect of contact time on the adsorption of patent blue V on the wTiHAp. Plain lines correspond to the theoretical fits obtained by using pseudo-second-order equation.

on both Ti content and the thermal treatment of wTiHAp powders. The highest capacity is obtained in the case 40TiHAp500, whereas the powder calcination at 500 °C is also very interesting in the regeneration adsorbent to decompose the adsorbed PB dye. It is noteworthy that certain attempts have also been made to fit the experimental data with the Langmuir and Freundlich models. Nevertheless, the Langmuir model is not adoptable (R^2 = 0.832), while a good fit is obtained with the Freundlich model. Parameters obtained from selected simulations are pasted in Table 3 and the corresponding fits are shown in Fig. 4. These results can be understood by taking into account the well-known complexation of PB dye at wTiHAp surface involving both sulfate and/or azo groups, but a limited affinity for charged negative surface such as titania or a large part of apatite surface is observed. Therefore, the sorption of PB does not follow the same trend as MB in terms of maximum capacity with increasing Ti content in samples. A higher PB sorption capacity of dried titania than that of received by 40TiHAp100 adsorbent is observed due to the large specific surface area of TiO_2 sample prepared with the ultrasonic assisted sol–gel method. However, their calcination at 500 °C affects the sorption process which 40TiHAp exhibits a good affinity with the coloring PB agent. The electrical nature of the 40TiHAp surface is still somewhat obscure but evidence suggests that probably a positive charge may be able to react with the negative charge of PB dye containing SO_4 groups. In addition, titania and apatite structures are also known to possess additional positive surface charges, which become significant with the acid pH. Feng et al. [17] have demonstrated a strong correlation between the acidity/alkalinity of TiO_2 and its adsorption capacity. Furthermore, the surface charge on the apatite layer is also contributed by the contamination with small amounts of Ti [24,25], which can affect the surface charge. It therefore explains the observed lower sorption of anionic patent blue as compared to the cationic methylene blue sorption. It must be noted that the sorption capacity does not seem to be directly dependent on the specific surface area but related to the chemical structure of dye including the ionic charge and the nature of chemical functions. Contrary to the cationic MB dye over all the pH range, the PB exhibits two negative sulfate groups and that should be interacted by the apatite surface and presumed to be positively charged. Therefore, our data reflect both the low affinity of calcined titania for PB sorption due to electrostatic repulsion with the oxygen-Ti and -SO_4 groups of PB dye, so the calcined TiO_2 at 500 °C attained a lower sorption capacity of PB than of pure HAp apatite.

Table 2 Kinetic rate constants (k_i) and adsorption capacities ($q_{e,i}$) as obtained for different models for the patent blue removal by wTiHAp powders.

			40TiHAp	25TiHAp	HAp	TiO_2
100 °C	Pseudo 1st order	k_1 (min^{-1})	0.037	0.076	0.043	0.020
		$q_{e,1}$ (mg g^{-1})	1.40	1.21	0.93	1.401
		R^2	0.94553	0.9286	0.8819	0.8232
	Pseudo 2nd order	k_2 (min^{-1})	0.112	0.203	0.236	0.106
		$q_{e,2}$ (g mg^{-1} min^{-1})	4.89	3.67	3.35	4.40
		R^2	0.9998	0.9998	0.9991	0.9998
500 °C	Pseudo 1st order	k_1 (min^{-1})	0.031	0.028	0.030	0.047
		$q_{e,1}$ (mg g^{-1})	1.230	1.245	1.439	3.40
		R^2	0.9242	0.85651	0.8756	0.8192
	Pseudo 2nd order	k_2 (min^{-1})	0.260	0.185	0.118	0.164
		$q_{e,2}$ (g mg^{-1} min^{-1})	4.59	3.49	3.19	2.76
		R^2	0.9998	0.9998	0.9998	0.9998

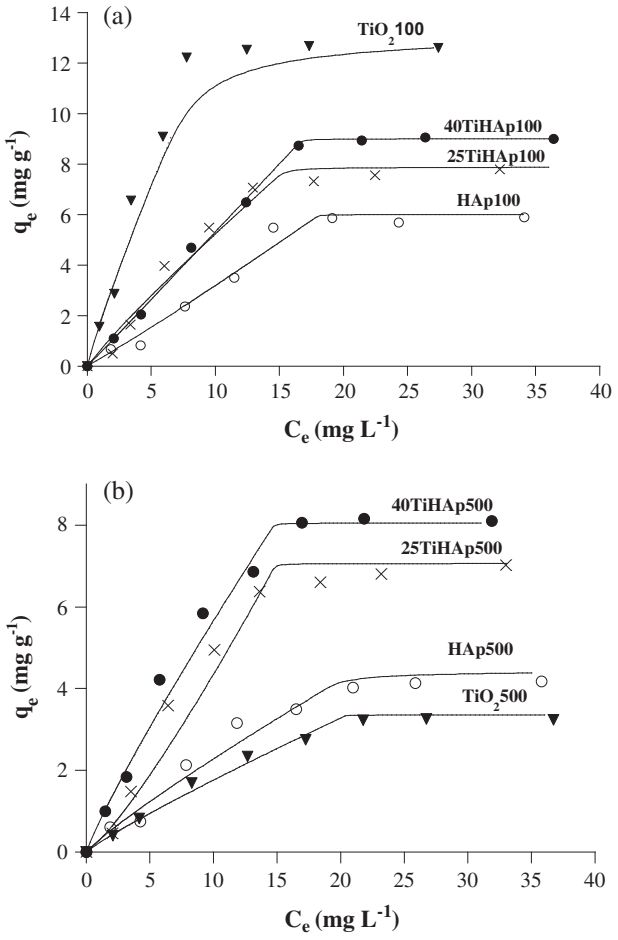

Fig. 4 Effect of the initial concentration of patent blue on its adsorption on the dried (a) and calcined (500 °C) (b) wTiHAp powders. Plain lines correspond to the theoretical fits obtained by using a Freundlich-derived equation.

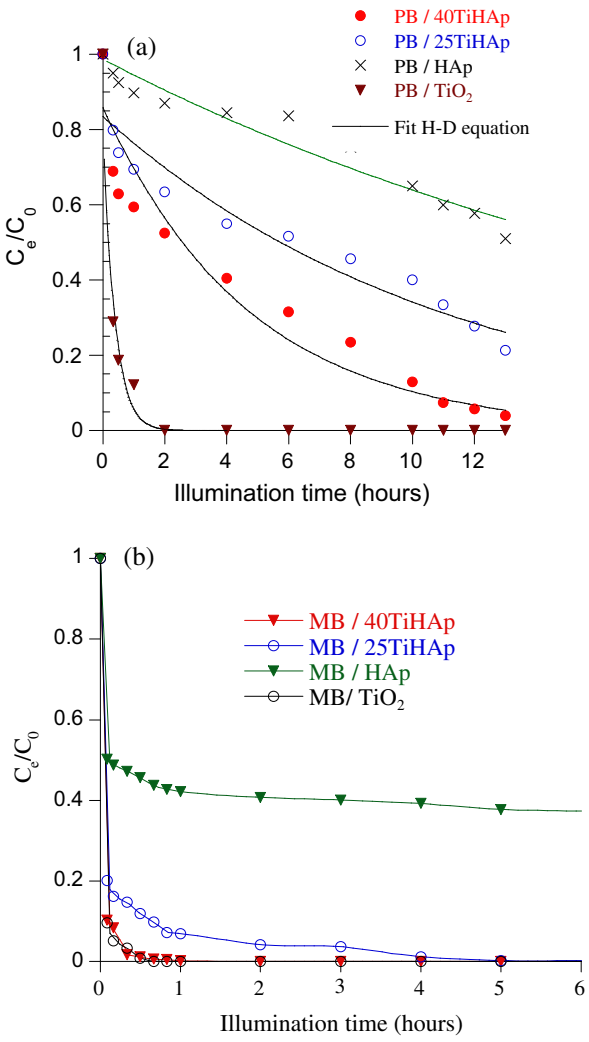

Fig. 5 Comparison of degradation kinetics between (a) patent blue and (b) methylene blue on wTiHAp catalysts.

Photodegradation process

The present section involves the photocatalytic degradation of the patent blue (PB) compared to the methyl blue (MB), employing heterogeneous photocatalytic process. Photocatalytic activity of 25TiHAp and 40TiHAp compared to titanium dioxide (TiO_2) and hydroxyapatite (HAp) as references has been investigated. An attempt has been made to study the effect of initial time, nature of catalyst, and concentration of dye on the photocatalytic degradation of patent blue. Fig. 5 shows that in the presence of wTiHAp catalysts, PB is less efficiently degraded compared to methylene blue. In fact, PB dye was fully degraded after 24 h, whereas 1 h was crucial to degrade the methylene blue under the same conditions, taking into consideration their chemical structures. The kinetics of the

Table 3 Adsorption constants related to Langmuir and Freundlich models.

Adsorbents		Exp. q_{max} (mg g^{-1})	Langmuir			Freundlich		
			q_L	β	R^2	$1/n$	K_f	R^2
100 °C	HAp	5.8	11.2	0.04	0.8763	0.98	9.46	0.9802
	25TiHAp	7.7	12.5	0.07	0.9254	0.90	9.51	0.9872
	40TiHAp	9.8	13.8	0.08	0.9305	0.92	9.93	0.9862
	TiO_2	12.0	13.7	0.08	0.9622	0.84	9.96	0.9918
500 °C	HAp		8.33	0.03	0.9345	0.89	9.48	0.9886
	25TiHAp		10.98	0.06	0.9207	0.90	9.44	0.9886
	40TiHAp		12.28	0.07	0.9401	0.88	9.97	0.9687
	TiO_2	3.30	5.26	0.05	0.9575	0.89	9.35	0.9939

Table 4 Rate constant and full degradation time of patent blue V degradation. Conditions: 20 mg/L of PB; pH 5.6 and ambient temperature.

	HAp	25TiHAp	40TiHAp	TiO_2
K_{app} (h^{-1})	0.03	0.09	0.21	2.71
Full degradation time (h)	>48	36	24	2

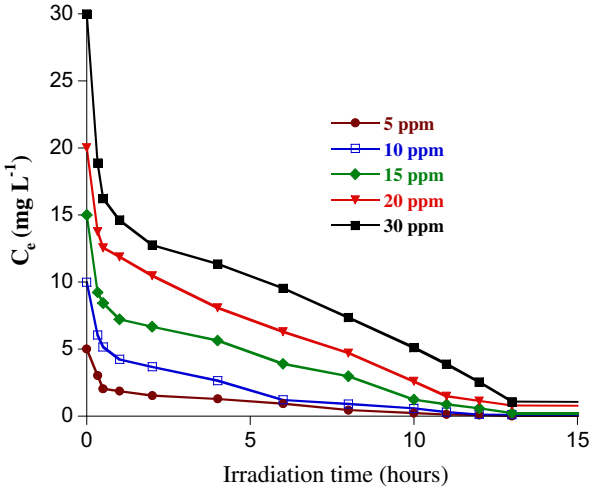

Fig. 6 Effect of initial concentration of PB dye on its degradation on 40TiHAp500 catalyst.

degradation reaction vary between PB and MB dyes. Both the dyes follow a Langmuir–Hinshelwood model based on the linear relation of the $\log(C/C_0)$ versus time. For PB photodegradation data, the k_{app} constant and the full degradation time are given in Table 4. It can be predicted that the significant difference in reaction rates might be due to the different structural features and Ti content in catalyst.

The photocatalytic oxidation kinetics of PB compounds is often simulated by Langmuir–Hinshelwood equation, which also covers the adsorption properties of the substrate on the photocatalyst surface. As shown in Table 4, the apparent first-order rate constant increases with TiO_2 content. The dependence of the patent blue disappearance on its initial concentration in its kinetics is shown in Fig. 6. It is noticeable that the residual concentration of PB into solution decreases as the irradiation time increases and the decomposition rate depends on the initial PB concentration. On the other hand, the presence of the catalyst under irradiation may induce different reactions such as photo-ionization, hemolytic breaking of chemical bonds with formation of different radical moieties, beyond hydroxyl radicals ($HO^{\bullet}$) themselves, which are the principal agents responsible for the oxidation of numerous aqueous organic contaminants [26,27]. Detailed reaction pathways have already been described in relatively more detail in most of the works on photodegradation reactions by using TiO_2 catalyst or titania derivate [29,30]. In our case, the kinetics of degraded products are documented, whereas their chromatographic peaks are plotted against the irradiation time (Fig. 7). Patent blue is absorbed in 8 min as retaining time

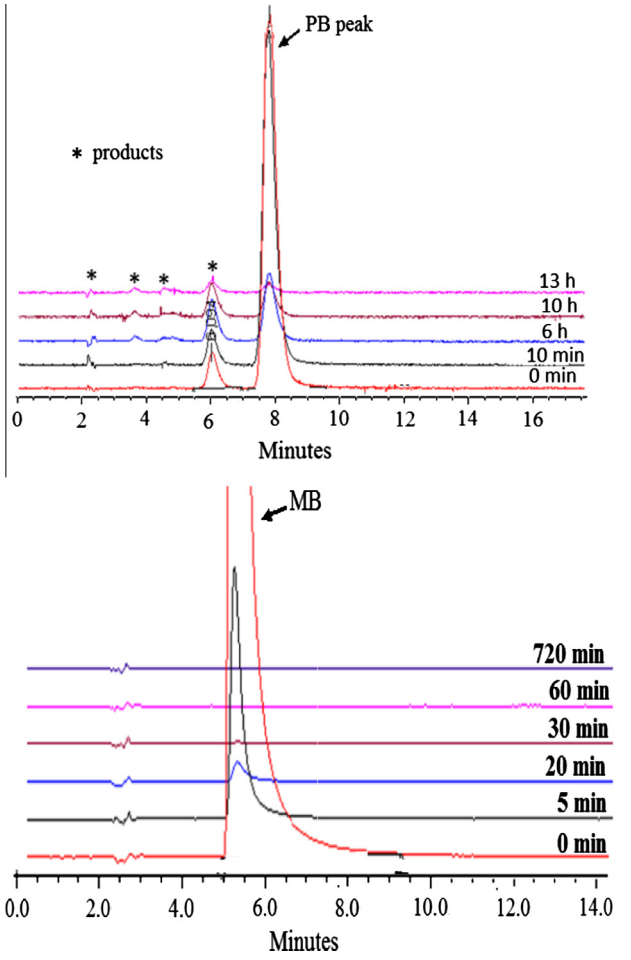

Fig. 7 HPLC curves of PB and MB degradation kinetics on 40TiHAp500 catalyst and their intermediate products.

and less detectable after 13 h of irradiation, while a few peaks are appeared contrary to MB degradation. Barka et al. [28] have detected a great number of intermediate compounds during the photocatalytic degradation of patent blue by supported TiO_2 and suggested the existence of various degradation routes, resulting in multi-step and interconnected pathways. However, the porous apatite structure can fix numerous by-products, knowing that the MB can discolor without degrading in accordance with R or S structures, but its HPLC-time of retention is always maintained well at 5 min with both the R or S configurations. The disappearance of their peaks in HPLC spectra with the absence of intermediate photoproducts proves that there is (i) a possible degradation instead of discoloration or (ii) a sorption of the blanched methylene dye onto apatite surface. From these hypotheses, it was recognized that major parts of degraded products were fixed by porous apatite. This fact sheds light on the reason that why no intermediate photoproducts have been detected in aqueous solution by photocatalytic decomposition of methylene blue compared to a few traces of degraded products within patent blue. Nishikawa [29] has demonstrated that hydroxyapatite is a photoactive catalyst and is a good support of fixing the intermediate products after methyl mercaptan photodegradation. Various studies consider that the hydroxyapatite is a good photoactive catalyst

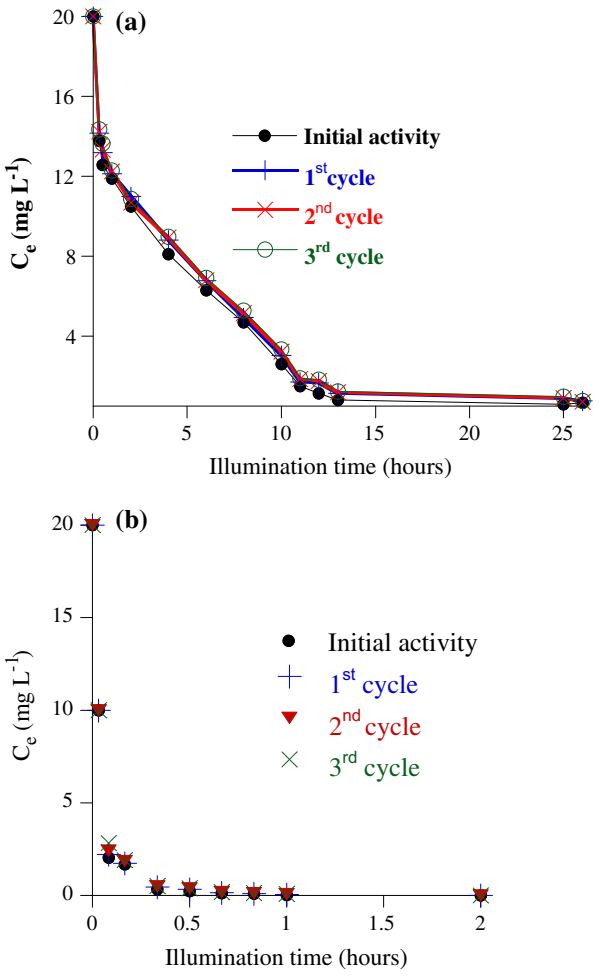

Fig. 8 Effect of regeneration (cycles 1–3) on photodegradation of (a) patent blue V and (b) methylene blue on 40TiHAp500 catalyst. The data presented here are concerned with only 3 cycles to better visualize the change in photodegradation activity. Initial concentration for both the dyes is C_0 = 20 ppm, dose = 2 g L^{-1}, T = 25 °C, without pH adjustment.

for a few organic pollutants [30–32]. In our case, the porous hydroxyapatite is considered as adsorbent instead photocatalyst linked to its low photocatalytic activity.

Regeneration

The results of the regeneration of the adsorbent are shown in Fig. 8. The 40TiHAp adsorbent/catalyst is separated from solution after dye sorption and degradation reactions, calcined at 500 °C, and then utilized as new adsorbent or catalyst to test that whether the catalyst undergoes any change in its original adsorbing and photocatalytic activities. This process has been carried out several times to achieve the effect of regeneration on the adsorption capacity of the resulting material. Thus, no apparent change in the adsorption capacity has been observed after several regenerations up to 5 cycles while the average loss in photodegradation activity during regeneration is found to about of 3% per cycle due to the change of the particles size.

Conclusions

Herein, wTiHAp nanocomposites prepared from natural phosphate and Ti-alkoxide were evaluated for the removal of the patent blue dye from aqueous solutions. The adsorption of PB was strongly related to the specific surface area of dried powders whereas the mineral surface charge appears a key parameter for the calcined powders. The extent of sorption and degradation of PB was significantly affected by the illumination time, the Ti content in the composites and the initial concentration of PB pollutant. Kinetic studies demonstrated that these two steps occur with different regimes, involving PB dimer adsorption but PB monomer photodegradation. Comparison with previous data on the removal of methylene blue suggests that the high negative charge of PB is detrimental to its interaction with the TiO_2 phase, resulting in a slower degradation rate. These results indicate that wTiHAp are promising nanocomposites for the removal of cationic dyes from contaminated waters.

Conflict of Interest

The authors have declared no conflict of interest.

Compliance with Ethics Requirements

This article does not contain any studies with human or animal subjects.

References

[1] Bhatia M, Goyal D. Analyzing remediation potential of wastewater through wetland plants: a review. Environ Prog Sustain Energy 2014;33:9–27.
[2] Padoley KV, Mudlair S, Pandey R. Heterocyclic nitrogenous pollutants in the in the environment and their treatment options. Bioresour Technol 2008;99:4029–43.
[3] Tang WZ, Zhang Z, Au H, Quintana MO, Torres DF. Photocatalytic degradation kinetics and mechanism of acid blue 40 by TiO_2/UV in aqueous solution. Environ Technol 1997;18:1–12.
[4] Faria PPC, Orfao JJM, Pereira MFR. Adsorption of anionic and cationic dyes on activated carbons with different surface chemistries. Water Res 2004;38:2043–52.
[5] Bouyarmane H, El Hanbali I, El Karbane M, Rami A, Saoiabi A, Saoiabi S, Masse S, Coradin T, Laghzizil A. Parameters influencing ciprofloxacin, ofloxacin, amoxicillin and sulfamethoxazole retention by natural and converted calcium phosphates. J Hazard Mater 2015;291:38–44.
[6] El Asri S, Laghzizil A, Coradin T, Saoiabi A, Alaoui A, M'hamedi R. Conversion of natural phosphate rock into mesoporous hydroxyapatite for heavy metals removal from aqueous solution. Colloid Surface A 2010;362:33–8.
[7] Saoiabi S, El Asri S, Laghzizil A, Saoiabi A, Ackerman JL, Coradin T. Lead and zinc removal from aqueous solutions by aminotriphosphonate-modified converted natural phosphates. Chem Eng J 2012;211–212:233–9.
[8] Achelhi K, Masse S, Laurent G, Roux C, Laghzizil A, Saoiabi A, Coradin T. Ultrasound-assisted synthesis of mesoporous zirconia-hydroxyapatite nanocomposites and their dual surface affinity for Cr^{3+}/$Cr_2O_7^{2-}$ ions. Langmuir 2011;27:15176–84.
[9] Ajmal A, Majeed I, Malik RN, Idriss H, Nadeem MA. Principles and mechanisms of photocatalytic dye degradation

on TiO_2 based photocatalysts: a comparative overview. RSC Adv 2014;4:37003–26.
[10] Gopi D, Govindaraju KM, Prakash-Victor CA, Kavitha L, Rajendiran N. Spectroscopic investigations of nanohydroxyapatite powders synthesized by conventional and ultrasonic coupled sol–gel routes. Spectrochim Acta Part A Mol Biomol Spectrosc 2008;70:1243–5.
[11] Mobasherpour I, Heshajin MS, Kazemzadeha A, Zakeri M. Synthesis of nanocrystalline hydroxyapatite by using precipitation method. J Alloys Compd 2007;430:330–3.
[12] Anmin H, Tong L, Ming L, Chengkang C, Huiqin L, Dali M. Preparation of nanocrystals hydroxyapatite/TiO_2 compound by hydrothermal treatment. Appl Catal B: Environ 2006;63:41–4.
[13] Nath S, Tripathi R, Basu B. Understanding phase stability, microstructure development and biocompatibility in calcium phosphate–titania composites, synthesized from hydroxyapatite and titanium powder mix. Mater Sci Eng, C 2009;29:97–107.
[14] Bouyarmane H, Saoiabi S, El Hanbali I, El Karbane M, Rami A, Masse S, Laghzizil A, Coradin T. Porous hydroxyapatite-TiO_2 nanocomposites from natural phosphates and their decolorization properties. Eur Phys J 2015;224:1863–71.
[15] Lemlikchi W, Drouiche N, Belaicha N, Oubagha N, Baaziz B, Mecherri MO. Kinetic study of the adsorption of textile dyes on synthetic hydroxyapatite in aqueous solution. J Ind Eng Chem 2015;32:233–7.
[16] Barka N, Qourzal S, Assabbane A, Nounah A, Ait-Ichou Y. Adsorption of disperse blue SBL dye by synthesized poorly crystalline hydroxyapatite. J Environ Sci 2008;20:1268–72.
[17] Feng J, Zhu J, Lv W, Li J, Yan W. Effect of hydroxyl group of carboxylic acids on the adsorption of acid red G and methylene blue on TiO_2. Chem Eng J 2015;269:316–22.
[18] Wan-Kuen J, Tayade RJ. Facile photocatalytic reactor development using nano-TiO_2 immobilized mosquito net and energy efficient UVLED for industrial dyes effluent treatment. J Environ Chem Eng 2016;4:19–327.
[19] Srihari V, Das A. The kinetics and thermodynamic studies of phenol-sorption on three agro-based carbons. Desalination 2008;225:220–34.
[20] Ho YS. Review of second-order models for adsorption systems. J Hazard Mater 2006;136:681–9.
[21] Konstantinou T, Albanis A. TiO_2 assisted photocatalytic degradation of azo dyes in aqueous solution: kinetic and mechanistic investigations: a review. Appl Catal B Environ 2004;49:1–14.
[22] Kim SH, Ngo HH, Shon HK, Vigneswaran S. Adsorption and photocatalysis kinetics of herbicide onto titanium oxide and powdered activated carbon. Sep Purif Technol 2008;58:335–42.
[23] Yang H, Masse S, Rouelle M, Aubry E, Li Y, Roux C, Journaux Y, Li L, Coradin T. Int J Environ Sci Technol 2015;12:1173.
[24] Castro Ribeiroa C, Gibsond I, Adolfo Barbosa M. The uptake of titanium ions by hydroxyapatite particles structural changes and possible mechanisms. Biomaterials 2006;227:1749–61.
[25] Layani JD, Mayer I, Cuisinier FJG. Carbonated hydroxyapatites precipitated in the presence of Ti. J Inorg Biochem 2000;81:57–63.
[26] Legrini O, Oliveros E, Braun AM. Photochemical processes for water treatment. Chem Rev 1993;93:671–98.
[27] Pedro JS, Valente S, Padilha PM, Florentino AO. Studies in the adsorption and kinetics of photodegradation of a model compound for heterogeneous photocatalysis onto TiO_2. Chemosphere 2006;64:1128–33.
[28] Barka N, Qourzal S, Assabbane A, Nounah A, Ait-Ichou Y. Photocatalytic degradation of patent blue V by supported TiO_2: kinetics, mineralization, and reaction pathway. Chem Eng Commun 2011;198:1233–43.
[29] Nishikawa H, Omamiuda K. Photocatalytic activity of hydroxyapatite for methyl mercaptane. J Mol Catal A: Chem 2002;179:193–200.
[30] Nishikawa H. Surface changes and radical formation on hydroxyapatite by UV irradiation for inducing photocatalytic activation. J Mol Catal A: Chem 2003;206:331–8.
[31] Nishikawa H. A high active type of hydroxyapatite for photocatalytic decomposition of dimethyl sulfide under UV irradiation. J Mol Catal A: Chem 2004;207:149–53.
[32] Bahdod A, El Asri S, Saoiabi A, Coradin T, Laghzizil A. Adsorption of phenol from an aqueous solution by selected apatite adsorbents: kinetic process and impact of the surface properties. Water Res 2009;43:313–8.